Two-Timescale Channel Estimation for Reconfigurable Intelligent Surface Aided Wireless Communications

Chen Hu, Linglong Dai, Shuangfeng Han, and Xiaoyun Wang

***Abstract*— Channel estimation is challenging for the reconfigurable intelligent surface (RIS)-aided wireless communications. Since the number of coefficients of the cascaded channel among the base station (BS), the RIS, and the user equipment (UE), is the product of the number of BS antennas, the number of RIS elements, and the number of UEs, the pilot overhead can be prohibitively high. In this paper, we propose a two-timescale channel estimation framework to exploit the property that the BS-RIS channel is high-dimensional but quasi-static, while the RIS-UE channel is mobile but low-dimensional. Specifically, to estimate the quasi-static BS-RIS channel, we propose a dual-link pilot transmission scheme, where the BS transmits downlink pilots and receives uplink pilots reflected by the RIS. Then, we propose a coordinate descent-based algorithm to recover the BS-RIS channel. Since the quasi-static BS-RIS channel is estimated less frequently than the mobile channel is, the average pilot overhead can be reduced from a long-term perspective. Although the mobile RIS-UE channel has to be frequently estimated in a small timescale, the associated pilot overhead is low thanks to its low dimension. Simulation results show that the proposed two-timescale channel estimation framework can achieve accurate channel estimation with low pilot overhead.**

***Index Terms*— Reconfigurable intelligent surface, channel estimation, pilot overhead.**

I. Introduction

THE emerging reconfigurable intelligent surface (RIS) has been recognized as a potential technology for the future 6G communications [1]. Different from conventional wireless communications where the propagation environment between the base station (BS) and the user equipment (UE) is considered uncontrollable, the RIS enables us to manipulate the wireless propagation environment by controlling the reflection coefficients on all RIS elements [2]. In the RIS-aided wireless communication system, accurate channel state information (CSI) is required to design the precoding matrix and the RIS reflection coefficients [3]. Consequently, it is of great importance to estimate the CSI in the RIS-aided wireless communication systems.

However, channel estimation for the RIS-aided wireless communication systems is a challenging problem due to the following two difficulties. Firstly, there are no active transmitters or receivers at the passive RIS, so the RIS can neither transmit nor receive pilots. By utilizing the active transceivers at the BS and UEs, most existing channel estimation methods only estimate the cascaded channel among the BS, the RIS and the UEs, i.e., the BS-RIS-UE cascaded channel [4], [5], where the BS-RIS-UE cascaded channel is the compound of the channel between the BS and the RIS (BS-RIS channel), and the channel between the RIS and the UEs (RIS-UE channel). Although most precoding schemes are based on the knowledge about the cascaded channel, there exist some precoding schemes [6] that require the individual CSI about both the BS-RIS channel and the RIS-UE channel. More importantly, the pilot overhead for the cascaded channel estimation methods is prohibitively high. A typical RIS-aided multi-user wireless communication system has a large number of BS antennas, a large number (e.g., dozens to hundreds) of RIS elements and dozens of UEs, while the pilot overhead of typical cascaded channel methods is the product of the number of RIS elements and the number of UEs [4], [5]. Consequently, the pilot overhead can be prohibitively high (e.g., hundreds to thousands) in practice, limiting the spectral efficiency and leading to channel estimation delays. This problem can be even more severe for high-mobility wireless communications. This motivates us to study low-overhead channel estimation methods that can estimate the channel within a short channel coherence time.

A. Prior Works

RIS-aided wireless communications are studied in [6]–[11], focusing on the joint optimization of the precoding matrix at the BS and the reflection coefficient vector at the RIS. The precoding problem for multi-user MIMO is proven to be non-convex and NP-hard [9], hence researchers tried to find the near-optimal joint-beamforming solutions for RIS-aided communications [10], [11]. In [12], [13], the authors reported

Manuscript received July 29, 2020; revised November 24, 2020, February 6, 2021, and March 22, 2021; accepted April 1, 2021. Date of publication April 12, 2021; date of current version November 18, 2021. This work was supported in part by the National Key Research and Development Program of China (Grant No. 2020YFB1807201), in part by the National Natural Science Foundation of China (Grant No. 62031019), and in part by the European Commission through the H2020-MSCA-ITN META WIRELESS Research Project under Grant 956256. The associate editor coordinating the review of this article and approving it for publication was B. Shim. *(Corresponding author: Xiaoyun Wang.)*

Chen Hu and Linglong Dai are with the Department of Electronic Engineering, Tsinghua University, Beijing 100084, China (e-mail: huc16@mails.tsinghua.edu.cn; daill@tsinghua.edu.cn).

Shuangfeng Han and Xiaoyun Wang are with China Mobile Research Institute, Beijing 100053, China (e-mail: hanshuangfeng@chinamobile.com; wangxiaoyun@chinamobile.com).

Color versions of one or more figures in this article are available at https://doi.org/10.1109/TCOMM.2021.3072729.

Digital Object Identifier 10.1109/TCOMM.2021.3072729

some important and interesting results in RIS-aided secure communications.

Up to now, the research on channel estimation for the RIS-aided communication systems is limited. There are only a few recent works on this topic [4], [5], [14]–[24], all of which estimate the BS-RIS-UE cascaded channel. In [4], only a single RIS element is turned on in one time slot, and the cascaded channel of this RIS element can be estimated. The channel estimation accuracy suffers from the degradation of the receiver signal-to-noise ratio (SNR) because all other RIS elements do not reflect the pilots. The authors in [5] designed a series of reflection coefficient vectors, and achieved a minimum variance unbiased (MVU) estimate of the cascaded channel. However, the pilot overhead for these schemes [4], [5] equals to the number of RIS elements multiplied by the number of UEs, which prohibits their application in a system with a large number of RIS elements. In [14], the authors propose an ingenious method to reduce the pilot overhead. The cascaded channel of the first UE is estimated at first and used as a reference channel. Then the cascaded channel of other UEs is estimated with reduced pilot overhead. However, the estimation is not accurate when the SNR is low. Another solution to reduce the pilot overhead is to use the sparse matrix factorization and matrix completion method if the channel exhibits the low-rank property [15], [16]. In addition, the spatial channel sparsity can be leveraged to reduce the pilot overhead based on the compressive sensing (CS) technique for the RIS-aided communication systems operating at high-frequency bands [17], [18]. [19], [20] use deep learning tools to solve the problem. However, these methods are not applicable in the general scenario where the channel is not low-rank or sparse.

B. Contributions

In this paper, by leveraging the two-timescale property of the channel, we propose a two-timescale channel estimation framework to significantly reduce the pilot overhead in RIS-aided wireless communication systems[1]. The contributions are summarized as follows:

1) We exploit the two-timescale channel property that the BS-RIS channel is quasi-static since the BS and the RIS are fixed, while the RIS-UE channel and the channel between the BS and the UEs (BS-UE channel) can change with time due to the mobility of the UEs. Then, we propose a two-timescale channel estimation framework to significantly reduce the pilot overhead. In this framework, the quasi-static BS-RIS with high dimension is estimated in a large timescale, while the mobile RIS-UE and BS-UE channels with low dimension are estimated in a small timescale.
2) To estimate the quasi-static BS-RIS channel, we propose a dual-link pilot transmission scheme, where the BS transmits downlink pilots and receives uplink pilots reflected by the RIS. Then, we propose a coordinate descent-based algorithm to recover the BS-RIS channel. Since the quasi-static BS-RIS channel is estimated less frequently than the mobile channel estimation for the UEs, the average pilot overhead associated with the former stage can be reduced from a long-term perspective.
3) For the mobile RIS-UE and the BS-UE channels, they can be easily estimated by the existing solutions such as the least square algorithm. Although they have to be frequently estimated in a small timescale, their dimension is smaller than that of the BS-RIS-UE cascaded channel, which still has to be frequently estimated in the existing cascaded channel estimation methods, so the associated pilot overhead can be significantly reduced.

[1]Simulation codes are provided to reproduce the results presented in this paper: http://oa.ee.tsinghua.edu.cn/dailinglong/publications/publications.html.

C. Organization and Notations

The remainder of the paper is organized as follows. In Section II, we introduce the model of the RIS-aided wireless communication systems. In Section III, we propose the two-timescale channel estimation framework, to exploit the property that the BS-RIS channel is high-dimensional but quasi-static, while the RIS-UE and BS-UE channels are mobile but low-dimensional. The proposed large-scale channel estimation method and the small-timescale channel estimation method is discussed in Section IV and Section V, respectively. Then, the pilot overhead and the computational complexity are analyzed in Section VI. We provide the simulation results in Section VII, and conclude this paper in Section VIII.

Notations: In this paper, light symbols, boldface lower-case symbols and upper-case symbols denote scalars, column vectors and matrices, respectively. $(\cdot)^*$ and $|\cdot|$ denote the conjugate and the amplitude, while $\|\cdot\|_0$, $\|\cdot\|_2$ and $\|\cdot\|_F$ denote the ℓ_0-norm, the ℓ_2-norm and the Frobenius norm, respectively. $(\cdot)^T$ and $(\cdot)^H$ are the transpose and the conjugate transpose, respectively. $\lceil x \rceil$ denotes the smallest integer that is greater than or equal to x. $\mathrm{diag}(\mathbf{x})$ is the diagonal matrix with the vector $\mathbf{x}$ on its diagonal. $\mathrm{vec}(\mathbf{X})$ is the vectorization of the matrix $\mathbf{X}$. $\odot$ is the Hadamard product. $\mathbf{I}_X$ is the $X \times X$ identity matrix. Finally, $\mathcal{CN}(\boldsymbol{\mu}, \boldsymbol{\Sigma})$ is the complex-valued Gaussian distribution with mean $\boldsymbol{\mu}$ and covariance $\boldsymbol{\Sigma}$.

II. System Model

We consider a RIS-aided wireless communication system as shown in Fig. 1. K UEs are served simultaneously by a BS with M antennas and a RIS with N elements. The uplink signal model is given by [3]

$$\mathbf{y} = \sum_{k=1}^{K} \left[\mathbf{G}\left(\boldsymbol{\phi} \odot \mathbf{f}_k\right) + \mathbf{h}_k\right] x_k + \mathbf{n}, \tag{1}$$

where $\mathbf{y} \in \mathbb{C}^{M\times 1}$ is the received signal at the BS, $\mathbf{G} \in \mathbb{C}^{M\times N}$ is the BS-RIS channel, $\boldsymbol{\phi} \in \mathbb{C}^{N\times 1}$ is the vector of reflection coefficients on the RIS elements, $\mathbf{f}_k \in \mathbb{C}^{N\times 1}$ is the channel between the RIS and the k-th UE, $\mathbf{h}_k \in \mathbb{C}^{M\times 1}$ is the direct channel between the BS and the k-th UE, $x_k \in \mathbb{C}$ is the transmitted signal from the k-th UE, and $\mathbf{n} \in \mathbb{C}^{M\times 1}$, $\mathbf{n} \sim \mathcal{CN}\left(\mathbf{0}, \sigma_n^2 \mathbf{I}_M\right)$ is the additive noise. We assume uncorrelated Rayleigh fading channels [25], i.e., $\mathbf{h}_k \sim \mathcal{CN}(\mathbf{0}, \rho_{h_k}\mathbf{I}_M)$,

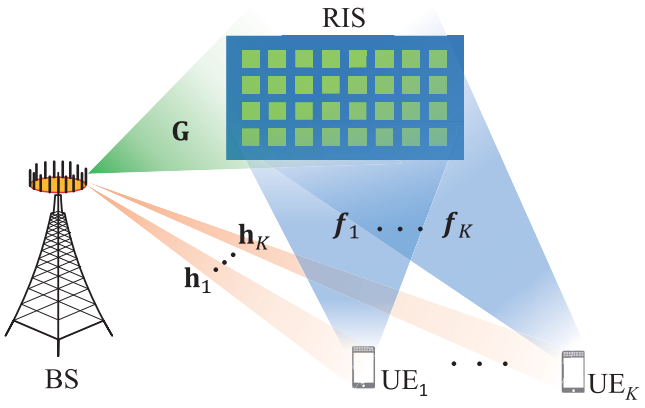

Fig. 1. The RIS aided wireless communication system.

$\mathrm{vec}(\mathbf{G}) \sim \mathcal{CN}(\mathbf{0}, \rho_g \mathbf{I}_{MN})$, $\mathbf{f}_k \sim \mathcal{CN}(\mathbf{0}, \rho_{f_k} \mathbf{I}_N)$, where ρ_{h_k}, ρ_g and ρ_{f_k} are the large-scale fading factors of these channels, respectively. Due to the RIS hardware limitations, the reflection coefficients should satisfy certain constraints. For example, as demonstrated in [26], the phases at RIS elements are controlled with 1-bit quantization, i.e., $\boldsymbol{\phi}(n) \in \{+1, -1\}$, $1 \le n \le N$.

The signal model (1) can be equivalently written as

$$\begin{aligned}\mathbf{y} &= \sum_{k=1}^{K} \left[\mathbf{G}\mathrm{diag}(\mathbf{f}_k)\boldsymbol{\phi} + \mathbf{h}_k\right] x_k + \mathbf{n} \\ &= \sum_{k=1}^{K} \left[\mathbf{C}_k\boldsymbol{\phi} + \mathbf{h}_k\right] x_k + \mathbf{n}, \end{aligned} \tag{2}$$

where the BS-RIS-UE cascaded channel is defined by

$$\mathbf{C}_k \triangleq \mathbf{G}\mathrm{diag}(\mathbf{f}_k), \quad k = 1, 2, \cdots, K, \tag{3}$$

which is the compound of the BS-RIS channel and the RIS-UE channel [15].

Most cascaded channel estimation methods in the literature are based on the uplink pilot transmission [5], [14], [15], [18]. In the t-th time slot, different UEs transmit different pilots $x_{k,t}$, while the RIS use the same reflection coefficient vector $\boldsymbol{\phi}_t$ to reflect the uplink pilots from all UEs. The received pilots at the BS can be modeled by

$$\begin{aligned}\mathbf{y}_t &= \sum_{k=1}^{K} \left[\mathbf{C}_k\boldsymbol{\phi}_t + \mathbf{h}_k\right] x_{k,t} + \mathbf{n}_t \\ &= \sum_{k=1}^{K} \mathbf{C}_k\boldsymbol{\phi}_t x_{k,t} + \sum_{k=1}^{K} \mathbf{h}_k x_{k,t} + \mathbf{n}_t. \end{aligned} \tag{4}$$

We repeat (4) for multiple time slots to received enough pilots, then the BS-RIS-UE cascaded channel $\{\mathbf{C}_k | 1 \le k \le K\}$ and the BS-UE channel $\{\mathbf{h}_k | 1 \le k \le K\}$ can be directly estimated by the methods in [4], [5]. Since the dimension of the received pilots should be no smaller than the dimension of the channels in [4], [5], the pilot overhead is extremely large to estimate the $(MNK + MK)$ coefficients in the BS-RIS-UE cascaded channel and the BS-UE direct channel for all the UEs.

III. The Proposed Two-Timescale Channel Estimation Framework

In this section, we propose a two-timescale channel estimation framework to leverage the two-timescale channel property. On one hand, the BS and the RIS are placed in fixed positions, so the BS-RIS channel $\mathbf{G}$ is quasi-static. We only need to estimate $\mathbf{G}$ in a large timescale, i.e., estimate $\mathbf{G}$ once over a long period of time. On the other hand, the RIS-UE channel and the BS-UE channel are time-varying due to the mobility of the UEs, so we need to estimate them in a small timescale, i.e., estimate them once in a short period of time.

To estimate the quasi-static BS-RIS channel, the main difficulty is that the RIS can neither transmit nor receive pilots because the RIS does not have active transceivers [2]. To overcome this difficulty, we propose a dual-link pilot transmission scheme. Specifically, the BS works at full-duplex mode [27]. The BS transmits pilots to the RIS via the downlink channel with a single antenna, and then the RIS reflects pilots back to the BS via the uplink channel with a set of pre-designed reflection coefficients, which will be explained later in detail. At the same time, the BS also receives pilots with the rest antennas. Though the self-interference can be severe in the full-duplex system, the self-interference mitigation techniques have been extensively studied to solve this problem, e.g., [27]–[29]. After the self-interference mitigation, the BS-RIS channel can be estimated based on the dual-link pilots which are received at the BS. Then, for the mobile RIS-UE and BS-UE channels, since they are low-dimensional, they can be estimated with a conventional uplink pilot transmission scheme and an LS-based algorithm.

Compared with the existing cascaded channel estimation methods, the pilot overhead can be significantly reduced. On one hand, the BS-RIS channel is high-dimensional but quasi-static. Since the quasi-static BS-RIS channel is estimated less frequently than the mobile channel estimation for the UEs, the average pilot overhead associated with the former stage can be reduced from a long-term perspective. On the other hand, the BS-UE and RIS-UE channels are mobile but low-dimensional. We estimate $\{\mathbf{h}_k, \mathbf{f}_k | 1 \le k \le K\}$ with only $(M + N)K$ coefficients, rather than estimating $\{\mathbf{h}_k, \mathbf{C}_k | 1 \le k \le K\}$ with $(M + MN)K$ coefficients by the cascaded channel estimation methods. The required pilot overhead can thus be significantly reduced.

The proposed channel estimation frame structure is exhibited in Fig. 2. At first, we estimate the high-dimensional quasi-static BS-RIS channel based on the proposed dual-link pilot transmission scheme. Then, in a small timescale, the low-dimensional mobile BS-UE and RIS UE channels are estimated based on the uplink pilots before data transmission.

IV. Quasi-Static BS-RIS Channel Estimation

In this section, we propose a dual-link pilot transmission scheme and a coordinate descent-based BS-RIS channel estimation algorithm to estimate the quasi-static BS-RIS channel.

A. Dual-Link Pilot Transmission

Before we start, we show that we cannot uniquely estimate the BS-RIS channel based on the pilot transmission model

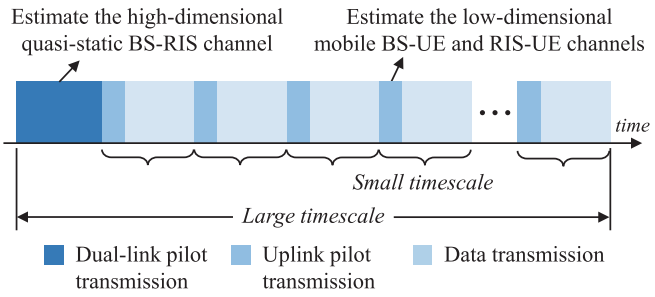

Fig. 2. The proposed two-timescale channel estimation frame structure.

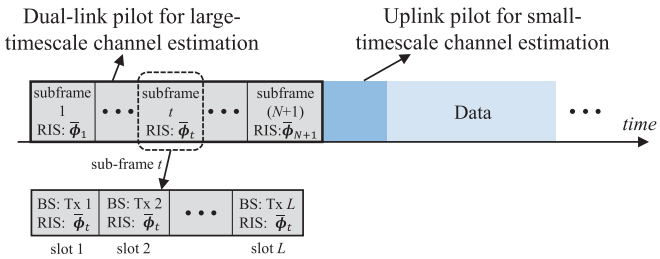

Fig. 3. Details of the proposed dual-link pilot transmission.

in (4), which is why we propose a novel dual-link pilot transmission scheme. Note that according to the definition of the cascaded channel in (3), for any non-zero $p_1, \cdots, p_N \in \mathbb{C}$,

$$\begin{aligned}\mathbf{C}_k &= \mathbf{G}\mathrm{diag}\left(\mathbf{f}_k\right) \\ &= \left(\mathbf{G}\begin{bmatrix} p_1 & & \\ & \ddots & \\ & & p_N \end{bmatrix}\right)\left(\begin{bmatrix} p_1^{-1} & & \\ & \ddots & \\ & & p_N^{-1} \end{bmatrix}\mathrm{diag}\left(\mathbf{f}_k\right)\right) \\ &= \mathbf{G}'\mathrm{diag}\left(\mathbf{f}_k'\right), \quad k = 1, 2, \cdots, K, \end{aligned} \tag{5}$$

where $\mathbf{G}' = \mathbf{G}\mathrm{diag}\left(\left[p_1, \cdots, p_N\right]^T\right)$, $\mathbf{f}_k' = \mathbf{f}_k \odot \left[p_1, \cdots, p_N\right]^T$. Equation (5) shows that the decomposition of the cascaded channel $\mathbf{C}_k$ is not unique. Therefore, no matter what pilots and no matter what reflection coefficients are used in the uplink pilot transmission in (4), both $\mathbf{G}, \{\mathbf{f}_k | 1 \le k \le K\}$ and $\mathbf{G}', \{\mathbf{f}_k' | 1 \le k \le K\}$ can lead to the same received pilots. As a result, we cannot uniquely estimate $\mathbf{G}$ and $\{\mathbf{f}_k | 1 \le k \le K\}$ based on the conventional uplink pilot transmission model in (4) [15]. So, we have to propose a pilot transmission scheme different from (4) to estimate the quasi-static BS-RIS channel.

In the proposed dual-link pilot transmission scheme, we do not need the UEs to transmit or receive pilots. We deploy a full-duplex BS in the RIS-aided communication system. The full-duplex wireless communication with RIS is regarded as a promising technology due to its high spectral efficiency. In [30], [31], the authors reported their recent results on resource allocation and beamforming design for RIS-aided full-duplex communications. In this system, the BS transmits pilots to the RIS via the downlink channel, and then the RIS reflects pilots back to the BS via the uplink channel.

Note that we cannot deliberately design one RIS beam that reflects the pilots to the direction of BS without channel knowledge. To solve this problem, we need multiple beams to exhaustively search through the whole space. In existing channel estimation works, the RIS can generate such beams without channel knowledge using orthogonal reflection coefficient vectors in different sub-frames [5]. As shown in Fig. 3, the proposed dual-link pilot transmission frame consists of $(N+1)$ sub-frames, and each sub-frame lasts for L time slots. In the t-th $(t = 1, 2, \cdots, N+1)$ sub-frame, the reflection coefficient vector at the RIS is $\bar{\phi}_t \in \mathbb{C}^{N \times 1}$. Based on the full-duplex MIMO architecture like [32], in the m_1-th $(m_1 = 1, 2, \cdots, L)$ time slot of the t-th sub-frame, the m_1-th BS antenna transmits a non-zero pilot $z_{m_1,t}$, and the rest $(M-1)$ BS antennas transmit zeros. The received pilots at the rest BS antennas can be written as

$$\begin{aligned}\bar{y}_{m_1,m_2,t} &= \left[\mathbf{g}_{m_2}^T \mathrm{diag}\left(\bar{\phi}_t\right)\mathbf{g}_{m_1} + s_{m_1,m_2}\right] z_{m_1,t} \\ &\quad + \bar{i}_{m_1,m_2,t} + \bar{n}_{m_1,m_2,t} \\ &= \left[\left(\mathbf{g}_{m_1} \odot \mathbf{g}_{m_2}\right)^T \bar{\phi}_t + s_{m_1,m_2}\right] z_{m_1,t} \\ &\quad + \bar{i}_{m_1,m_2,t} + \bar{n}_{m_1,m_2,t}, \\ &\quad m_2 = 1, 2, \cdots, M, m_2 \ne m_1, \end{aligned} \tag{6}$$

where $m_1 \ne m_2$. $\bar{y}_{m_1,m_2,t} \in \mathbb{C}$ is the received pilot at the m_2-th BS antenna, $\mathbf{g}_{m_2}^T \triangleq \mathbf{G}\left(m_2, :\right) \in \mathbb{C}^{1 \times N}$, $\mathbf{g}_{m_1} \triangleq \mathbf{G}\left(m_1, :\right)^T \in \mathbb{C}^{N \times 1}$.

Since the pilot transmission from BS to RIS and the reflection from RIS to BS are in exactly the same frequency band and happen simultaneously, the downlink channel and the uplink channel are reciprocal [33]. Note that the channel reciprocity means the same propagation environment for uplink and downlink. It does not mean that the arrival beam and the departure beam at the RIS are the same. Since $\mathbf{G}$ denotes BS-RIS channel matrix, $\mathbf{g}_{m_2}^T$, $\mathbf{g}_{m_1}^T$ are row vectors that denote the uplink channels from the RIS to the m_2-th and to the m_1-th BS antenna, respectively. Thanks to the channel reciprocity, the column vector $\mathbf{g}_{m_1}$ can be used to express the downlink channel from the m_1-th BS antenna to the RIS. The term s_{m_1,m_2} is used to represent the environmental reflection, since some objects other than the RIS elements can also reflect the pilot sent by the m_1-th BS antenna to the m_2-th RIS antenna. $\bar{i}_{m_1,m_2,t}$ is the self-interference after mitigation, which will be explained later. Finally, $\bar{n}_{m_1,m_2,t} \sim \mathcal{CN}\left(0, \sigma_n^2\right)$ is the received noise at the m_2-th BS antenna.

The self-interference $\bar{i}_{m_1,m_2,t}$ is mainly caused by the direct transmission from the m_1-th BS antenna to the m_2-th BS antenna when the BS is working at the full-duplex mode. In a typical full-duplex system, the self-interference can be even larger than the desired signal (e.g., 110 dB larger than the desired signal [27]) before mitigation. However, the self-interference suppression methods have been extensively studied to solve the problem, e.g., [27]–[29]. In [27], the authors reported that the interference can be mitigated to as low as about only 3 dB higher than the receiver noise with their self-interference mitigation method. Therefore, we assume $\bar{i}_{m_1,m_2,t} \sim \mathcal{CN}\left(0, \sigma_i^2\right)$ after the self-interference mitigation, where there is no considerable difference in orders of magnitude between σ_i^2 and σ_n^2. It is true that the self-interference suppression will result in increased hardware complexity at the

BS. It is still an open topic to study the RIS-aided full-duplex system in the future.

Denote the index tuple set $\mathcal{S} \triangleq \{(m_1, m_2) \,|1 \leq m_1 \leq L, 1 \leq m_2 \leq M, m_1 \neq m_2\}$. After $(N+1)$ sub-frames, we can get all the received pilots $\{\bar{y}_{m_1,m_2,t} | \, (m_1, m_2) \in \mathcal{S}, 1 \leq t \leq N+1\}$ in the dual-link pilot transmission frame. For a given $(m_1, m_2) \in \mathcal{S}$, we collect the received pilots corresponding to the m_1-th transmit antenna and the m_2-th receive antenna throughout $(N+1)$ sub-frames, to define

$$\bar{\mathbf{y}}_{m_1,m_2}^T \triangleq [\bar{y}_{m_1,m_2,1}, \bar{y}_{m_1,m_2,2}, \cdots, \bar{y}_{m_1,m_2,N+1}]. \quad (7)$$

Then, by substituting the dual-link pilot model (6) into (7), and assuming the transmitted pilot is $z_{m_1,t} = \sqrt{P_{\mathrm{BS}}}$ without loss of generality, where P_{BS} is the transmitted power of the BS, we can write the model in the vector form:

$$\begin{aligned} \bar{\mathbf{y}}_{m_1,m_2}^T &= \Big\{ \left(\mathbf{g}_{m_1} \odot \mathbf{g}_{m_2}\right)^T \left[\bar{\boldsymbol{\phi}}_1, \bar{\boldsymbol{\phi}}_2, \cdots, \bar{\boldsymbol{\phi}}_{N+1}\right] \\ &\quad + s_{m_1,m_2} \mathbf{1}_{1\times(N+1)} \Big\} \sqrt{P_{\mathrm{BS}}} + \bar{\mathbf{i}}_{m_1,m_2}^T + \bar{\mathbf{n}}_{m_1,m_2}^T \\ &= \sqrt{P_{\mathrm{BS}}} \mathbf{w}_{m_1,m_2}^T \begin{bmatrix} \mathbf{1}_{1\times(N+1)} \\ \bar{\boldsymbol{\Phi}} \end{bmatrix} + \bar{\mathbf{i}}_{m_1,m_2}^T + \bar{\mathbf{n}}_{m_1,m_2}^T, \end{aligned} \quad (8)$$

where we define the vector of unknown variables by

$$\mathbf{w}_{m_1,m_2} \triangleq \begin{bmatrix} s_{m_1,m_2} & \left(\mathbf{g}_{m_1} \odot \mathbf{g}_{m_2}\right)^T \end{bmatrix}^T, \quad (9)$$

and $\bar{\boldsymbol{\Phi}} = \left[\bar{\boldsymbol{\phi}}_1, \bar{\boldsymbol{\phi}}_2, \cdots, \bar{\boldsymbol{\phi}}_{N+1}\right] \in \mathbb{C}^{N\times(N+1)}$, $\mathbf{1}_{1\times(N+1)}$ is a row vector with all elements equal to 1, $\bar{\mathbf{i}}_{m_1,m_2} = [\bar{i}_{m_1,m_2,1}, \cdots, \bar{i}_{m_1,m_2,N+1}]^T$, $\bar{\mathbf{n}}_{m_1,m_2} = [\bar{n}_{m_1,m_2,1}, \cdots, \bar{n}_{m_1,m_2,N+1}]^T$. In (8), $\mathbf{w}_{m_1,m_2}$ consists of $N+1$ unknown coefficients to be estimated, including 1 coefficient associated with the environmental reflection and N coefficients associated with the RIS. Thus, the dimension of $\mathbf{y}_{m_1,m_2}$ should be at least $N+1$ to solve $\mathbf{w}_{m_1,m_2}$, which is why we need $N+1$ sub-frames.

Denote $\mathbf{F} \triangleq \begin{bmatrix} \mathbf{1}_{1\times(N+1)} \\ \bar{\boldsymbol{\Phi}} \end{bmatrix}$. Since we consider the 1-bit phase-shift RIS, we should choose the elements of $\bar{\boldsymbol{\Phi}}$ from $\{+1, -1\}$ and make $\mathbf{F}$ invertible. Therefore, (8) becomes

$$\bar{\mathbf{y}}_{m_1,m_2}^T = \sqrt{P_{\mathrm{BS}}} \mathbf{w}_{m_1,m_2}^T \mathbf{F} + \bar{\mathbf{i}}_{m_1,m_2}^T + \bar{\mathbf{n}}_{m_1,m_2}^T. \quad (10)$$

B. The Proposed Coordinate Descent-Based Channel Estimation Algorithm

Given the received dual-link pilots, we estimate the quasi-static BS-RIS channel in three stages. Firstly, we divide the problem into N independent subproblems, where each subproblem is to estimate the channel between the BS and a single RIS element. Secondly, initial estimates are calculated for each subproblem. Thirdly, the BS-RIS channel estimates are iteratively optimized via a coordinate descent approach.

1) Problem Division: In the first stage, for all $(m_1, m_2) \in \mathcal{S}$, based on the model (10), we can easily obtain an estimate of $\mathbf{w}_{m_1,m_2}$ defined in (9) by

$$\begin{aligned} \hat{\mathbf{w}}_{m_1,m_2}^T &\triangleq [\hat{s}_{m_1,m_2} \quad a_{m_1,m_2,1} \quad a_{m_1,m_2,2} \quad \cdots \quad a_{m_1,m_2,N}] \\ &= \frac{1}{\sqrt{P_{\mathrm{BS}}}} \bar{\mathbf{y}}_{m_1,m_2}^T \mathbf{F}^{-1}, \end{aligned} \quad (11)$$

where $\hat{s}_{m_1,m_2}$, $a_{m_1,m_2,1}$, $\cdots$, $a_{m_1,m_2,N}$ denote the elements of $\hat{\mathbf{w}}_{m_1,m_2}$.

By substituting (8) into (11), we have

$$\begin{aligned} &[\hat{s}_{m_1,m_2} \quad a_{m_1,m_2,1} \quad a_{m_1,m_2,2} \quad \cdots \quad a_{m_1,m_2,N}] \\ &= \left[s_{m_1,m_2} \quad \left(\mathbf{g}_{m_1} \odot \mathbf{g}_{m_2}\right)^T \right] + \frac{\left(\bar{\mathbf{i}}_{m_1,m_2}^T + \bar{\mathbf{n}}_{m_1,m_2}^T\right) \mathbf{F}^{-1}}{\sqrt{P_{\mathrm{BS}}}}. \end{aligned} \quad (12)$$

Therefore, $a_{m_1,m_2,n}$ is an estimate of $g_{m_1,n} g_{m_2,n}$, with

$$\begin{aligned} a_{m_1,m_2,n} &= g_{m_1,n} g_{m_2,n} + \varepsilon_{m_1,m_2,n}, \\ n &= 1, 2, \cdots, N, \end{aligned} \quad (13)$$

where $g_{m,n} = \mathbf{g}_m(n) = \mathbf{G}(m, n)$ is the channel between the m-th BS antenna and the n-th RIS element, $\varepsilon_{m_1,m_2,n}$ is the error.

Now that for a specific n, $1 \leq n \leq N$, the variables $\{a_{m_1,m_2,n} | \, (m_1, m_2) \in \mathcal{S}\}$ are dependent to the channel coefficients between the BS and the n-th RIS element, i.e., $\{g_{m,n} | 1 \leq m \leq M\}$, but independent to the channel coefficients related to other RIS elements. That is to say, the problem of estimating the quasi-static BS-RIS channel can thus be divided into N independent subproblems, where the n-th subproblem is to estimate the channel coefficients related to the n-th RIS element $\{g_{m,n} | 1 \leq m \leq M\}$ from $\{a_{m_1,m_2,n} | \, (m_1, m_2) \in \mathcal{S}\}$. Since $|\mathcal{S}| \geq M$ is required to guarantee the solvability of the subproblems, we need to have $L \geq 2$.

In the following stages, we will estimate the quasi-static BS-RIS channel by solving the N subproblems respectively. For a given n, we formulate the n-th subproblem as

$$\hat{g}_{1,n}, \hat{g}_{2,n}, \cdots, \hat{g}_{M,n} = \arg \min_{g_{1,n}, \cdots, g_{M,n}} J_n\left(g_{1,n}, \cdots, g_{M,n}\right), \quad (14)$$

where

$$J_n\left(g_{1,n}, \cdots, g_{M,n}\right) \triangleq \sum_{(m_1,m_2)\in\mathcal{S}} \left| a_{m_1,m_2,n} - g_{m_1,n} g_{m_2,n} \right|^2. \quad (15)$$

2) Calculate Initial Channel Estimates: The goal of the second stage is to calculate initial channel estimates for the subproblems in (14). The initial estimates are coarse and easy to calculate, which will help the iterative refinement in the third stage converge faster. Specifically, we pick $1 \leq m_1 < m_2 \leq L$ and $m_3 \neq m_1, m_2$. The initial estimates $\hat{g}_{1,n}^{(0)}, \hat{g}_{2,n}^{(0)}, \cdots, \hat{g}_{M,n}^{(0)}$ for the n-th subproblem are calculated by

$$\hat{g}_{m_1,n}^{(0)} \leftarrow \sqrt{\frac{a_{m_1,m_2,n} a_{m_1,m_3,n}}{a_{m_2,m_3,n}}}, \quad (16)$$

$$\hat{g}_{m',n}^{(0)} \leftarrow \frac{a_{m_1,m',n}}{\hat{g}_{m_1,n}^{(0)}}, \; 1 \leq m' \leq M, m' \neq m_1. \quad (17)$$

3) Coordinate Descent-Based Iterative Refinement: In the third stage, we propose a coordinate descent-based algorithm to refine the coarse channel estimates and find the accurate estimates of the quasi-static BS-RIS channel, to solve the subproblems in (14). There are multiple outer iterations in the coordinate descent based algorithm, each of which consists of M inner iterations. The key idea is that, in each outer iteration, the estimates of all the M coefficients are refined from the first one to the last one. In each inner iteration, we refine the estimate of one of the M coefficients while fixing the estimates of the rest $(M-1)$ coefficients.

To be specific, in the i-th outer iteration, we loop for $1 \leq m \leq M$. In the m-th inner iteration, we refine the estimate of $g_{m,n}$ but fix the estimate of other $M-1$ channel coefficients at $g_{1,n}^{(i,m)}, \cdots, g_{m-1,n}^{(i,m)}, g_{m+1,n}^{(i,m)}, \cdots, g_{M,n}^{(i,m)}$, where

$$g_{m',n}^{(i,m)} \triangleq \begin{cases} \hat{g}_{m',n}^{(i)}, & m' < m, \\ \hat{g}_{m',n}^{(i-1)}, & m' > m, \end{cases} \tag{18}$$

which means that $\hat{g}_{1,n}^{(i)}, \cdots, \hat{g}_{m-1,n}^{(i)}$ have been refined before refining $\hat{g}_{m,n}$ in the current outer iteration, and $\hat{g}_{m+1,n}^{(i-1)}, \cdots, \hat{g}_{M,n}^{(i-1)}$ have been refined in the $(i-1)$-th outer iteration. Using these notations, the inner-iteration problem of refining the estimate of $g_{m,n}$ is formulated as

$$\hat{g}_{m,n}^{(i)} = \underset{g_{m,n}}{\operatorname{argmin}} J_n\left(g_{1,n}^{(i,m)}, \cdots, g_{m-1,n}^{(i,m)}, g_{m,n}, g_{m+1,n}^{(i,m)}, \cdots, g_{M,n}^{(i,m)}\right). \tag{19}$$

As a univariate optimization problem, the close-form solution for (19) can be derived by solving $\frac{\partial J_n}{\partial g_{m,n}} = \frac{\partial J_n}{\partial g_{m,n}^*} = 0$. According to the definition of the objective function f_n in (15), the partial derivatives are given by

$$\begin{aligned} \frac{\partial J_n}{\partial g_{m,n}} &= \frac{\partial}{\partial g_{m,n}} \sum_{(m,m')\in\mathcal{S}} \left| a_{m,m',n} - g_{m,n} g_{m',n}^{(i,m)} \right|^2 \\ &\quad + \frac{\partial}{\partial g_{m,n}} \sum_{(m',m)\in\mathcal{S}} \left| a_{m',m,n} - g_{m',n}^{(i,m)} g_{m,n} \right|^2 \\ &= g_{m,n}^* \left(\sum_{(m,m')\in\mathcal{S}} \left| g_{m',n}^{(i,m)} \right|^2 + \sum_{(m',m)\in\mathcal{S}} \left| g_{m',n}^{(i,m)} \right|^2 \right) \\ &\quad + \sum_{(m,m')\in\mathcal{S}} a_{m,m',n}^* g_{m',n}^{(i,m)} \\ &\quad + \sum_{(m',m)\in\mathcal{S}} a_{m',m,n}^* g_{m',n}^{(i,m)}, \end{aligned} \tag{20}$$

and similarly

$$\begin{aligned} \frac{\partial J_n}{\partial g_{m,n}^*} &= g_{m,n} \left(\sum_{(m,m')\in\mathcal{S}} \left| g_{m',n}^{(i,m)} \right|^2 + \sum_{(m',m)\in\mathcal{S}} \left| g_{m',n}^{(i,m)} \right|^2 \right) \\ &\quad + \sum_{(m,m')\in\mathcal{S}} a_{m,m',n} \left(g_{m',n}^{(i,m)} \right)^* \\ &\quad + \sum_{(m',m)\in\mathcal{S}} a_{m',m,n} \left(g_{m',n}^{(i,m)} \right)^*. \end{aligned} \tag{21}$$

Therefore, the close-form solution to (19) is obtained by $\frac{\partial J_n}{\partial g_{m,n}} = \frac{\partial J_n}{\partial g_{m,n}^*} = 0$, which yields to

$$\hat{g}_{m,n}^{(i)} = \frac{\sum\limits_{(m,m')\in\mathcal{S}} a_{m,m',n} \left(g_{m',n}^{(i,m)} \right)^* + \sum\limits_{(m',m)\in\mathcal{S}} a_{m',m,n} \left(g_{m',n}^{(i,m)} \right)^*}{\sum\limits_{(m,m')\in\mathcal{S}} \left| g_{m',n}^{(i,m)} \right|^2 + \sum\limits_{(m',m)\in\mathcal{S}} \left| g_{m',n}^{(i,m)} \right|^2}. \tag{22}$$

Finally, we verify the convergence of the coordinate descent-based channel estimation algorithm. From (15), we can see that $J_n\left(g_{1,n}^{(i,m)}, \cdots, g_{m-1,n}^{(i,m)}, g_{m,n}, g_{m+1,n}^{(i,m)}, \cdots, g_{M,n}^{(i,m)}\right)$ is convex with regard to $g_{m,n}$. As a result, after we update the estimate of $g_{m,n}$ according to (22), the value of J_n will decrease or keep unchanged, i.e.,

$$\begin{aligned} &J_n\left(g_{1,n}^{(i)}, \cdots, g_{m-1,n}^{(i)}, g_{m,n}^{(i-1)}, g_{m+1,n}^{(i-1)}, \cdots, g_{M,n}^{(i-1)}\right) \\ &\quad \geq J_n\left(g_{1,n}^{(i)}, \cdots, g_{m-1,n}^{(i)}, g_{m,n}^{(i)}, g_{m+1,n}^{(i-1)}, \cdots, g_{M,n}^{(i-1)}\right). \end{aligned} \tag{23}$$

Therefore, we have

$$\begin{aligned} J_n\left(g_{1,n}^{(i-1)}, \cdots, g_{M,n}^{(i-1)}\right) &\geq \cdots \geq J_n\left(\cdots, g_{m,n}^{(i)}, g_{m+1,n}^{(i-1)}, \cdots\right) \\ &\geq \cdots \geq J_n\left(g_{1,n}^{(i)}, \cdots, g_{M,n}^{(i)}\right), \end{aligned} \tag{24}$$

$$J_n\left(g_{1,n}^{(0)}, \cdots, g_{M,n}^{(0)}\right) \geq \cdots \geq J_n\left(g_{1,n}^{(I_{\max})}, \cdots, g_{M,n}^{(I_{\max})}\right) \geq 0. \tag{25}$$

The values of J_n are bounded and monotonic during the proposed coordinate descent-based channel estimation algorithm, hence the estimate of BS-RIS channel $\{g_{m,n} | 1 \leq m \leq M\}$ will finally converge.

The coordinate descent-based channel estimation algorithm is summarized in **Algorithm 1**. In Steps 1-6, we divide the quasi-static channel estimation problem into N independent subproblems, each of which estimates the channel between the BS and one specific RIS element. In Steps 7-17, the subproblems are solved respectively using the coordinate descent method. As described in Steps 10-15, the outer iterations are run until a well-fit solution is found or the number of outer iterations reaches $I_{\max}$. In Step 13, we refine the m-th channel coefficients in the inner iterations. Finally, the algorithm will find an estimate of the quasi-static BS-RIS channel.

V. Mobile RIS-UE and BS-UE Channel Estimation

Given the estimate of the quasi-static BS-RIS channel, we can estimate the mobile RIS-UE channel $\{\mathbf{f}_k | 1 \leq k \leq K\}$ and the BS-UE channel $\{\mathbf{h}_k | 1 \leq k \leq K\}$. Since the mobile channels are low-dimensional, they can be estimated with the conventional uplink pilot transmission scheme and an LS-based algorithm.

A. Uplink Pilot Transmission

To estimate the mobile RIS-UE and BS-UE channels, we follow the conventional uplink pilot transmission scheme [5]. The uplink pilot transmission frame consists of τ_0 sub-frames, and each sub-frame lasts for K time slots. In the t-th sub-frame ($t = 1, 2, \cdots, \tau_0$), the reflection coefficient vector

Algorithm 1 The Proposed Coordinate Descent-Based Channel Estimation Algorithm

Input: Received pilots $\{\bar{y}_{m_1,m_2,n}|\,(m,m')\in\mathcal{S},1\le n\le N\}$, the transmitted power $P_{\rm BS}$, the termination threshold ϵ, the maximal number of outer iterations $I_{\max}$, matrix $\mathbf{F}$ in (10).

Output: Estimated coefficients $\{\hat{g}_{m,n}|1\le m\le M,1\le n\le N\}$ of the BS-RIS channel.

for $m_1=1:L$ **do**
  for $m_2=1:M, m_2\neq m_1$ **do**
    $\bar{\mathbf{y}}^T_{m_1,m_2}\triangleq[\bar{y}_{m_1,m_2,1},\bar{y}_{m_1,m_2,2},\cdots,\bar{y}_{m_1,m_2,N+1}]$.
    $[\hat{s}_{m_1,m_2}\ \ a_{m_1,m_2,1}\ \ a_{m_1,m_2,2}\ \ \cdots\ \ a_{m_1,m_2,N}]=\frac{1}{\sqrt{P_{\rm BS}}}\bar{\mathbf{y}}^T_{m_1,m_2}\mathbf{F}^{-1}$.
  end for
end for
for $n=1:N$ **do**
  Initialize $\hat{g}^{(0)}_{1,n},\hat{g}^{(0)}_{2,n},\cdots,\hat{g}^{(0)}_{M,n}$ according to (16)-(17).
  $i=0$.
  while $J_n\left(\hat{g}^{(i)}_{1,n},\cdots,\hat{g}^{(i)}_{M,n}\right)>\epsilon$ **and** $i<I_{\max}$ **do**
    $i\leftarrow i+1$.
    for $m=1:M$ **do**
      Calculate $\hat{g}^{(i)}_{m,n}$ according to (22).
    end for
  end while
  $\hat{g}_{m,n}=\hat{g}^{(i)}_{m,n},1\le m\le M$.
end for
return $\{\hat{g}_{m,n}|1\le m\le M,1\le n\le N\}$

at the RIS is $\tilde{\boldsymbol{\phi}}_t\in\mathbb{C}^{N\times1}$. The elements of the reflection coefficient vector are randomly drawn from $\{+1,-1\}$. During the K time slots in a sub-frame, the UEs transmit uplink pilot sequences, i.e., $\mathbf{x}_k\in\mathbb{C}^{K\times1}$, $k=1,2,\cdots,K$. In order to distinguish the pilots from different UEs, we assign orthogonal pilot sequences to different UEs, i.e.,

$$\mathbf{x}^H_{k_1}\mathbf{x}_{k_2}=\begin{cases}KP_{\rm UE}, & k_1=k_2,\\ 0, & k_1\neq k_2,\end{cases}\tag{26}$$

with $P_{\rm UE}$ denoting the transmitted power of each UE.

In the t-th sub-frame, based on (2), we write the multi-slot pilot transmission model by

$$\mathbf{Y}_t=\sum_{k=1}^{K}\left[\mathbf{G}\mathrm{diag}\left(\mathbf{f}_k\right)\tilde{\boldsymbol{\phi}}_t+\mathbf{h}_k\right]\mathbf{x}^T_k+\mathbf{N}_t,\tag{27}$$

where $\mathbf{Y}_t\in\mathbb{C}^{M\times K}$ is the matrix of received pilots at the BS. Each column of $\mathbf{Y}_t$ is the received pilots in a single time slot. $\mathbf{N}_t\in\mathbb{C}^{M\times K}$ is the noise.

Then, by right multiplying the conjugate of the pilot sequences, we can distinguish the channels of different UEs:

$$\begin{aligned}\tilde{\mathbf{y}}_{k,t}&=\frac{1}{KP_{\rm UE}}\mathbf{Y}_t\mathbf{x}^*_k\\&=\frac{1}{KP_{\rm UE}}\sum_{k'=1}^{K}\left[\mathbf{G}\mathrm{diag}\left(\mathbf{f}_{k'}\right)\tilde{\boldsymbol{\phi}}_t+\mathbf{h}_{k'}\right]\mathbf{x}^T_{k'}\mathbf{x}^*_k+\frac{\mathbf{N}_t\mathbf{x}^*_k}{KP_{\rm UE}}\\&=\left[\mathbf{G}\mathrm{diag}\left(\tilde{\boldsymbol{\phi}}_t\right)\mathbf{f}_k+\mathbf{h}_k\right]+\tilde{\mathbf{n}}_{k,t}\\&=\mathbf{A}_t\begin{bmatrix}\mathbf{f}_k\\ \mathbf{h}_k\end{bmatrix}+\tilde{\mathbf{n}}_{k,t},\quad k=1,2,\cdots,K,\end{aligned}\tag{28}$$

where $\tilde{\mathbf{n}}_{k,t}=\frac{\mathbf{N}_t\mathbf{x}^*_k}{KP_{\rm UE}}$, and

$$\mathbf{A}_t\triangleq\left[\mathbf{G}\mathrm{diag}\left(\tilde{\boldsymbol{\phi}}_t\right)\ \mathbf{I}_M\right].\tag{29}$$

In (28), $\tilde{\mathbf{y}}_{k,t}\in\mathbb{C}^{M\times1}$ is the equivalent received pilot for the k-th UE, $\left[\mathbf{f}^T_k,\mathbf{h}^T_k\right]^T\in\mathbb{C}^{(M+N)\times1}$ is the vector of all coefficients of the mobile channels of the k-th UE. Since the number of received pilots must be no smaller than the dimension of the mobile channels, i.e., $\tau_0M\ge M+N$, we have $\tau_0\ge\tau_{\min}=\lceil\frac{M+N}{M}\rceil$. Then, by collecting the equivalent received pilots in τ_0 sub-frames, we have

$$\tilde{\mathbf{y}}_k=\mathbf{A}\begin{bmatrix}\mathbf{f}_k\\ \mathbf{h}_k\end{bmatrix}+\tilde{\mathbf{n}}_k,\quad k=1,2,\cdots,K,\tag{30}$$

where $\tilde{\mathbf{y}}_k\triangleq\left[\tilde{\mathbf{y}}^T_{k,1},\tilde{\mathbf{y}}^T_{k,2},\cdots,\tilde{\mathbf{y}}^T_{k,\tau_0}\right]^T$, $\mathbf{A}\triangleq\left[\mathbf{A}^T_1,\mathbf{A}^T_2,\cdots,\mathbf{A}^T_{\tau_0}\right]^T$, and $\tilde{\mathbf{n}}_k\triangleq\left[\tilde{\mathbf{n}}^T_{k,1},\tilde{\mathbf{n}}^T_{k,2},\cdots,\tilde{\mathbf{n}}^T_{k,\tau_0}\right]^T$.

B. LS-Based Channel Estimation Algorithm

In (30), $\mathbf{A}$ is determined by the exact quasi-static channel $\mathbf{G}$ and the series of reflection coefficients $\left\{\tilde{\boldsymbol{\phi}}_t\middle|1\le t\le\tau_0\right\}$. The reflection coefficients $\left\{\tilde{\boldsymbol{\phi}}_t\middle|1\le t\le\tau_0\right\}$ are predesigned, while the exact value of $\mathbf{G}$ is not known to us. So we can only use $\hat{\mathbf{G}}$ which is estimated in the quasi-static channel estimation. Similar to (29), we define $\hat{\mathbf{A}}$ based on $\hat{\mathbf{G}}$

$$\hat{\mathbf{A}}\triangleq\begin{bmatrix}\hat{\mathbf{G}}\mathrm{diag}\left(\tilde{\boldsymbol{\phi}}_1\right)\ \mathbf{I}_M\\ \vdots\qquad\vdots\\ \hat{\mathbf{G}}\mathrm{diag}\left(\tilde{\boldsymbol{\phi}}_{\tau_0}\right)\ \mathbf{I}_M\end{bmatrix}.\tag{31}$$

Finally, we have the least square (LS) estimate of the mobile channels

$$\begin{bmatrix}\hat{\mathbf{f}}_k\\ \hat{\mathbf{h}}_k\end{bmatrix}=\hat{\mathbf{A}}^{\dagger}\tilde{\mathbf{y}}_k=\left(\hat{\mathbf{A}}^H\hat{\mathbf{A}}\right)^{-1}\hat{\mathbf{A}}^H\tilde{\mathbf{y}}_k,\quad k=1,2,\cdots,K,\tag{32}$$

where $\hat{\mathbf{f}}_k$ and $\hat{\mathbf{h}}_k$ are the estimates of the RIS-UE channel and the BS-UE channel of the k-th UE, respectively.

VI. Pilot Overhead and Computational Complexity

A. Pilot Overhead

In the quasi-static channel estimation, there are MN coefficients in the BS-RIS channel that need to be estimated in a large timescale. We use $(N+1)$ sub-frames, each of which consists of L time slots. To make sure that the number of received pilot is larger than the number of channel coefficients, we need $L\ge2$. The associated pilot overhead is $\tau_1=(N+1)L$, proportional to L. In the mobile channel estimation stage, there are NK coefficients in the RIS-UE channel and MK coefficients in the BS-UE channel that need to be estimated in a small timescale. Since the BS gets MK pilot measurements in one sub-frame of K time slots, we need at least $\lceil\frac{(M+N)K}{MK}\rceil=\lceil\frac{N}{M}\rceil+1$ sub-frames. Thus,

TABLE I

PILOT OVERHEAD COMPARISON OF DIFFERENT CHANNEL ESTIMATION SCHEMES

Channel estimation scheme	Applicable scenario	Minimum pilot overhead
Proposed two-timescale	General	$\frac{2(N+1)}{\alpha} + K\lceil\frac{N}{M}\rceil + K$
MVU [5]	General	$NK + K$
Multi-user [14]	General	$K+N+\max\left\{K-1, \lceil\frac{(K-1)N}{M}\rceil\right\}$
CS [17]	Sparse	$\mathcal{O}(KS\log N)$

the pilot overhead for the small-timescale channel estimation is $\tau_2 = K\lceil\frac{N}{M}\rceil + K$.

In the proposed two-time channel estimation framework, the quasi-static BS-RIS channel is estimated in a large timescale. As a result, we need to average the pilot overhead of large-timescale channel estimation depending on how frequently the BS-RIS channel is estimated. Specifically, let T_L and T_S denote the channel coherence time of the large-timescale channel and the small-timescale channel, respectively, and $T_L = \alpha T_S$ with $\alpha \gg 1$. During a time period of T_S, the average pilot overhead is calculated by $\tau = \frac{T_S}{T_L}\cdot\tau_1 + \tau_2 = \frac{(N+1)L}{\alpha} + K\lceil\frac{N}{M}\rceil + K$. The minimum required pilot overhead is $\frac{2(N+1)}{\alpha} + K\lceil\frac{N}{M}\rceil + K$ when $L = 2$.

In Table I, we compare the pilot overhead of the proposed two-timescale channel estimation with the MVU channel estimation [5], the multi-user channel estimation [14], and a typical CS-based sparse channel estimation [17]. The proposed two-timescale channel estimation and the schemes in [5], [14] are able to solve the general channel estimation problem without any sparse or low-rank assumptions about the channel. The pilot overhead of the proposed two-timescale channel estimation is lower than $NK + K$ in [5], and lower than $K + N + \max\left\{K-1, \lceil\frac{(K-1)N}{M}\rceil\right\}$ in [14] when $\alpha > 2$. Besides, CS-based channel estimation schemes such as [17] are applicable only to sparse channels in high-frequency wireless communications. The pilot overhead of [17] can be significantly reduced when the sparsity level S is small and N is large.

Figs. 4-6 illustrate the relation between the pilot overhead and M, N, K, where $\alpha = 4$. In Fig. 4, for both the proposed channel estimation scheme and the method in [14], the pilot overhead decreases as the number of BS antennas increases because the BS can get more measurements of uplink pilots in a time slot with more antennas. Figs. 5-6 show that the more RIS elements and the more UEs, the more pilots are required. In addition, we can see that the pilot overhead of the proposed two-timescale channel estimation framework is lower than the multi-user channel estimation method in [14], and significantly lower than the minimum variance unbiased (MVU) estimator [5], by leveraging the two-timescale channel property.

From the pilot overhead analysis, we can see that α is a key factor that contributes to the pilot reduction. When the BS-RIS channel varies much more slowly than the RIS-UE channel and BS-UE channel do ($\alpha \gg 1$), the advantage of the proposed method is significant. On the contrary, when the BS-RIS channel also varies fast ($\alpha \approx 1$), e.g., in scenarios where the BS or RIS are on vehicles, the proposed method will not achieve significant pilot reduction.

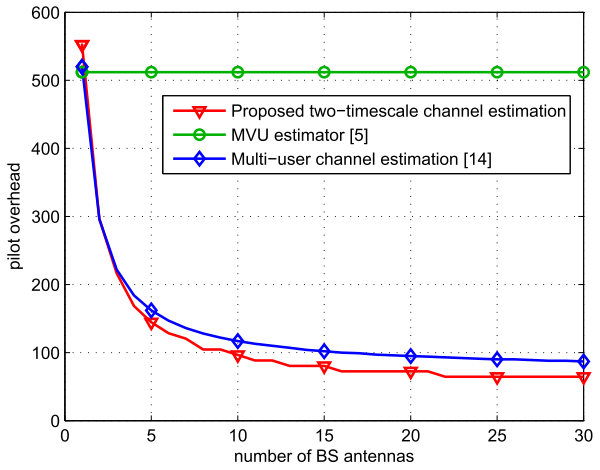

Fig. 4. The pilot overhead against M, where $N = 64$, $K = 8$, $L = 2$.

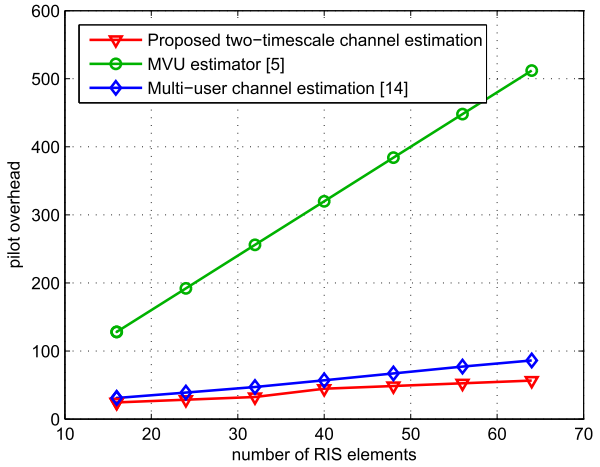

Fig. 5. The pilot overhead against N, where $M = 32$, $K = 8$, $L = 2$.

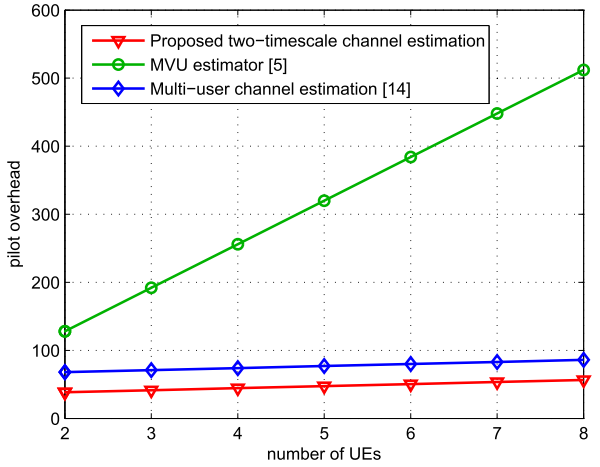

Fig. 6. The pilot overhead against K, where $M = 32$, $N = 64$, $L = 2$.

B. Computational Complexity

In the quasi-static channel estimation, we can calculate the matrix inversion $\mathbf{F}^{-1}$ at first with the computational

complexity $\mathcal{O}\left(N^3\right)$. Then, the computation complexity of **Algorithm 1** mainly lies in the vector-matrix multiplication in Step 4 and the operations in Step 14. The computational complexity for vector-matrix multiplication in Step 4 is $\mathcal{O}\left(N^2\right)$. In Step 13, it takes $\mathcal{O}\left(M\right)$ calculations when $m \leq L$, and $\mathcal{O}\left(L\right)$ when $m > L$, so the computational complexity of Steps 12-14 is $\mathcal{O}\left(ML\right)$. Considering the number of iterations, the computational complexity of **Algorithm 1** is $\mathcal{O}\left(N^3 + MLN^2 + MLNI_{\max}\right)$. In the mobile channel estimation, the computational complexity is determined by that of the LS channel estimation in (32), which is $\mathcal{O}\left(\left(M+N\right)^3 + \left(M+N\right)^2 K\right)$.

VII. Simulations

A. Simulation Setup

In our simulations, $M = 32$, $N = 256$, $K = 8$, and $L = 2$. The large-scale fading is modeled as $\rho_{h_k} = \rho_0 \left(\frac{d_{h_k}}{d_0}\right)^{-\alpha_h}$, $\rho_g = \rho_0 \left(\frac{d_g}{d_0}\right)^{-\alpha_g}$, $\rho_{f_k} = \rho_0 \left(\frac{d_{f_k}}{d_0}\right)^{-\alpha_f}$, where $\rho_0 = -20$ dB is the large-scale fading factor at the reference distance of $d_0 = 1$ m, and we set $\alpha_h = 2.2$, $\alpha_g = 2.1$ and $\alpha_f = 4.2$, which are also adopted in the simulations in [14]. The BS-RIS distance is $d_g = 20$ m, the BS-UE distance is $d_{h_k} = 30$ m, and the RIS-UE distance is $d_{f_k} = 20$ m. The transmit power of the BS is 10 times that of a UE. The proposed two-timescale channel estimation consists of the large-timescale channel estimation and the small-timescale channel estimation, which are influenced by different noises. For the dual-link pilot transmission in the large-timescale channel estimation, we define the signal-to-interference-plus-noise ratio by

$$\mathrm{SINR}_L \triangleq \frac{P_{\mathrm{BS}}\rho_g^2}{\sigma_i^2 + \sigma_n^2}, \tag{33}$$

where the after-mitigation self-interference level is set to be 2 times as strong as the receiver noise, i.e., $\sigma_{\mathrm{SI}}^2 = 2\sigma_n^2$ [27]. While for the uplink pilot transmission in the small-timescale channel estimation, we define the signal-to-noise ratio by

$$\mathrm{SNR}_S = \frac{P_{\mathrm{UE}}\rho_r\rho_g}{\sigma_n^2}. \tag{34}$$

B. Simulation Results

First of all, we examine the convergence of the proposed large-timescale channel estimation algorithm by simulations. We randomly generate 100 channels and run the entire channel estimation procedure for each of them. In each channel estimation, we need to solve $N = 256$ subproblems (14). For each subproblem, we can evaluate the normalized value of the objective function by

$$\bar{J}_n^{(i)} \triangleq \frac{J_n\left(\hat{g}_{1,n}^{(i)}, \cdots, \hat{g}_{M,n}^{(i)}\right)}{\mathbb{E}\left\{J_n\left(0, \cdots, 0\right)\right\}}, \quad i = 1, \cdots, I_{\max}, \tag{35}$$

so we can record how the value of $\bar{J}_n^{(i)}$ decreases with i for the $100N = 25,600$ independent subproblems. In Fig. 7, we show the means and standard deviations of $\bar{J}_n^{(i)}$ by the curves of error bars, under $\mathrm{SINR}_L = 0$ dB, $\mathrm{SINR}_L = 10$ dB and $\mathrm{SINR}_L = 20$ dB, respectively. As shown in Fig. 7, the value of the objective function drops as the coordinate descent-based algorithm proceeds. In no more than 5 outer iterations, the value of the objective function converges to a small mean value. Moreover, the error bar in Fig. 7 is short. Thus, we can conclude that the convergence of the proposed coordinate descent-based algorithm is fast and stable.

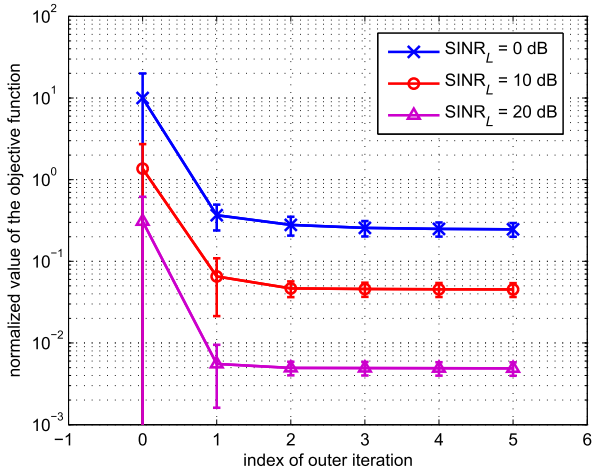

Fig. 7. The convergence of the coordinate descent-based channel estimation algorithm, where $M = 32$, $N = 256$, $K = 8$, $L = 2$.

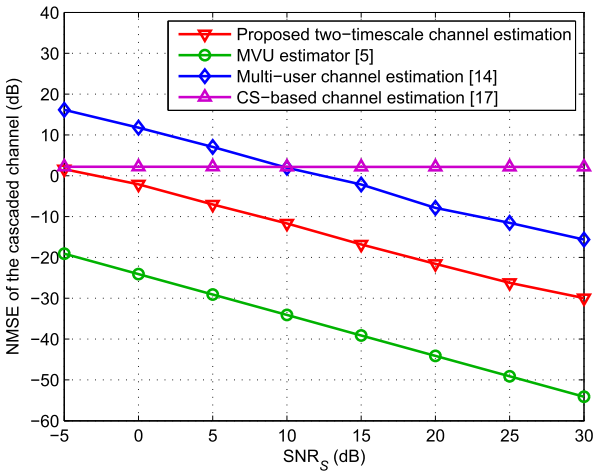

Fig. 8. The NMSE for the cascaded channel against uplink SNR, where $M = 32$, $N = 256$, $K = 8$, $L = 2$.

In Figs. 8-9, we investigate the normalized mean square error (NMSE) performance. The channels are Rayleigh channels described in Section II. To compare the NMSE performance with the existing cascaded channel estimation methods, we should also calculate the estimate of the cascaded channel $\{\mathbf{C}_k | 1 \leq k \leq K\}$ by $\hat{\mathbf{C}}_k = \hat{\mathbf{G}}\mathrm{diag}\left(\hat{\mathbf{f}}_k\right)$, $1 \leq k \leq K$. The NMSE of the cascaded channel is defined by

$$\mathrm{NMSE}_C \triangleq \frac{\mathbb{E}\left\{\sum_{k=1}^{K}\left\|\hat{\mathbf{C}}_k - \mathbf{C}_k\right\|_F^2\right\}}{\mathbb{E}\left\{\sum_{k=1}^{K}\left\|\mathbf{C}_k\right\|_F^2\right\}}, \tag{36}$$

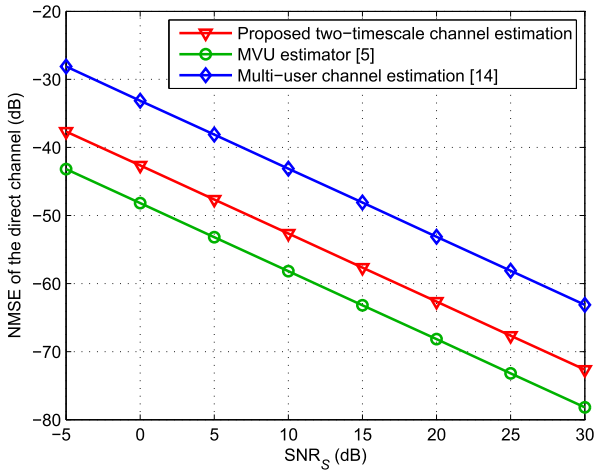

Fig. 9. The NMSE for the direct channel against uplink SNR, where $M = 32$, $N = 256$, $K = 8$, $L = 2$.

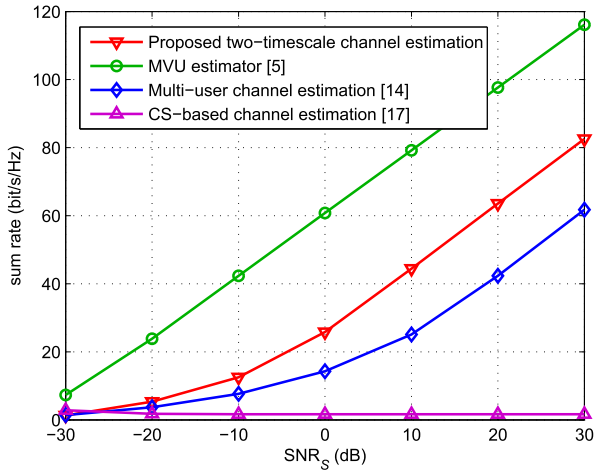

Fig. 10. The sum-rate comparison with regard to uplink SNR, where $M = 32$, $N = 256$, $K = 8$, $L = 2$.

while the NMSE of the BS-UE channel is

$$\mathrm{NMSE}_h \triangleq \frac{\mathbb{E}\left\{\sum_{k=1}^{K}\left\|\hat{\mathbf{h}}_k - \mathbf{h}_k\right\|_2^2\right\}}{\mathbb{E}\left\{\sum_{k=1}^{K}\|\mathbf{h}_k\|_2^2\right\}}. \tag{37}$$

Fig. 8 shows the NMSE of the cascaded channel against the SNR, while Fig. 9 shows the NMSE of the BS-UE channel against the SNR. In Fig. 8, we can see that the NMSE decreases as SNR becomes large except for the CS-based channel estimation [17]. This is because [17] cannot find a meaningful channel estimate when the sparsity is not available in Rayleigh channels. The proposed channel estimation method can achieve lower NMSE than that in [14]. The MVU channel estimation [5] is more accurate, but it is mainly because the pilot overhead is an order of magnitude higher than that of our proposed method.

Fig. 10 studies the sum-rate performance against SNR, to show how the RIS-aided communication system works with different CSI. Different channel estimation schemes are used

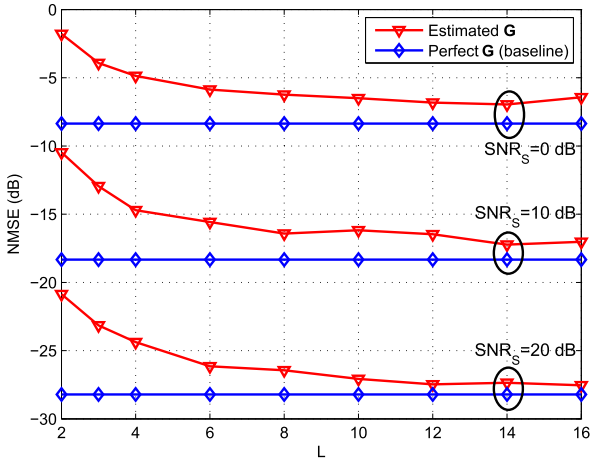

Fig. 11. The NMSE for the cascaded channel with regard to L, where $M = 32$, $N = 128$, $K = 8$.

to acquire CSI for the joint optimization of the precoding matrix at the BS and the reflection coefficient vector at the RIS. The sum-rate is calculated by

$$R = \sum_{k=1}^{K} \log_2\left(1 + \mathrm{SINR}_k^u\right), \tag{38}$$

where SINR_k^u is the signal-to-interference-plus-noise ratio for the k-th user after the joint optimization. Considering the constraint that the RIS reflection coefficients are in $\{+1, -1\}$, we adopt a cross entropy optimization-based precoding scheme similar to that in [34] to jointly optimize the precoding matrix at the BS and the reflection coefficient vector at the RIS. The result is consistent with Figs. 8-9, that the proposed channel estimation method can outperform the method in [14]. The sum-rate performance of the CS-based channel estimation [17] is poor because the channel sparsity is not available.

In Fig. 11, we show that the NMSE is also influenced by L. L is the number of time slots in each sub-frame in the quasi-static BS-RIS channel estimation stage. We draw the baseline curves by assuming that the BS-RIS channel $\mathbf{G}$ are estimated accurately without error, and then the RIS-UE channel is estimated by the proposed method. We can observe that when L becomes large, the NMSE results decrease and approach the baseline. This is because the NMSE results are determined by both the large-timescale channel estimation and the small-timescale channel estimation. The BS-RIS channel is estimated more accurately at the expense of larger L, but the NMSE cannot break the baseline's limits because the RIS-UE channel estimation can also introduce some error.

VIII. Conclusions

In this paper, we have proposed a two-timescale channel estimation framework for the RIS-aided wireless communication systems. The key idea of the framework is to exploit the two-timescale property, which means that the BS-RIS channel is high-dimensional but quasi-static, while the RIS-UE channel and the BS-UE channel are mobile but low-dimensional.

We reveal that the pilot overhead can be significantly reduced by exploiting the two-timescale channel property. For the quasi-static BS-RIS channel, the average pilot overhead can be reduced from a long-term perspective since it is not estimated frequently. For the mobile RIS-UE and BS-UE channels that have to be frequently estimated in a small timescale, their dimension is smaller than that of the cascaded channel, so the pilot overhead can be significantly reduced. Simulation results show that the proposed two-timescale channel estimation framework can achieve accurate channel estimation with low pilot overhead.

REFERENCES

[1] Z. Zhang *et al.*, "6G wireless networks: Vision, requirements, architecture, and key technologies," *IEEE Veh. Technol. Mag.*, vol. 14, no. 3, pp. 28–41, Sep. 2019.

[2] E. Basar, M. Di Renzo, J. De Rosny, M. Debbah, M.-S. Alouini, and R. Zhang, "Wireless communications through reconfigurable intelligent surfaces," *IEEE Access*, vol. 7, pp. 116753–116773, Aug. 2019.

[3] S. Hu, F. Rusek, and O. Edfors, "Beyond massive MIMO: The potential of data transmission with large intelligent surfaces," *IEEE Trans. Signal Process.*, vol. 66, no. 10, pp. 2746–2758, May 2018.

[4] D. Mishra and H. Johansson, "Channel estimation and low-complexity beamforming design for passive intelligent surface assisted MISO wireless energy transfer," in *Proc. IEEE Int. Conf. Acoust., Speech Signal Process. (ICASSP)*, Brighton, U.K., May 2019, pp. 4659–4663.

[5] T. L. Jensen and E. De Carvalho, "An optimal channel estimation scheme for intelligent reflecting surfaces based on a minimum variance unbiased estimator," in *Proc. IEEE Int. Conf. Acoust., Speech Signal Process. (ICASSP)*, Barcelona, Spain, May 2020, pp. 5000–5004.

[6] C. Huang, A. Zappone, M. Debbah, and C. Yuen, "Achievable rate maximization by passive intelligent mirrors," in *Proc. IEEE Int. Conf. Acoust., Speech Signal Process. (ICASSP)*, Calgary, AB, Canada, Apr. 2018, pp. 3714–3718.

[7] J. Ye, S. Guo, and M.-S. Alouini, "Joint reflecting and precoding designs for SER minimization in reconfigurable intelligent surfaces assisted MIMO systems," *IEEE Trans. Wireless Commun.*, vol. 19, no. 8, pp. 5561–5574, Aug. 2020.

[8] T. Bai, C. Pan, Y. Deng, M. Elkashlan, A. Nallanathan, and L. Hanzo, "Latency minimization for intelligent reflecting surface aided mobile edge computing," *IEEE J. Sel. Areas Commun.*, vol. 38, no. 11, pp. 2666–2682, Nov. 2020.

[9] Z.-Q. Luo and S. Zhang, "Dynamic spectrum management: Complexity and duality," *IEEE J. Sel. Topics Signal Process.*, vol. 2, no. 1, pp. 57–73, Feb. 2008.

[10] H. Guo, Y.-C. Liang, J. Chen, and E. G. Larsson, "Weighted sum-rate maximization for reconfigurable intelligent surface aided wireless networks," *IEEE Trans. Wireless Commun.*, vol. 19, no. 5, pp. 3064–3076, May 2020.

[11] Z. Zhang and L. Dai, "A joint precoding framework for wideband reconfigurable intelligent surface-aided cell-free network," *IEEE Trans. Signal Process.*, 2021.

[12] H. Yang *et al.*, "Intelligent reflecting surface assisted anti-jamming communications: A fast reinforcement learning approach," *IEEE Trans. Wireless Commun.*, vol. 20, no. 3, pp. 1963–1974, Mar. 2021.

[13] H. Yang, Z. Xiong, J. Zhao, D. Niyato, L. Xiao, and Q. Wu, "Deep reinforcement learning-based intelligent reflecting surface for secure wireless communications," *IEEE Trans. Wireless Commun.*, vol. 20, no. 1, pp. 375–388, Jan. 2021.

[14] Z. Wang, L. Liu, and S. Cui, "Channel estimation for intelligent reflecting surface assisted multiuser communications: Framework, algorithms, and analysis," *IEEE Trans. Wireless Commun.*, vol. 19, no. 10, pp. 6607–6620, Oct. 2020.

[15] Z.-Q. He and X. Yuan, "Cascaded channel estimation for large intelligent metasurface assisted massive MIMO," *IEEE Wireless Commun. Lett.*, vol. 9, no. 2, pp. 210–214, Feb. 2020.

[16] K. Ardah, S. Gherekhloo, A. L. F. de Almeida, and M. Haardt, "TRICE: A channel estimation framework for RIS-aided millimeter-wave MIMO systems," *IEEE Signal Process. Lett.*, vol. 28, pp. 513–517, Feb. 2021.

[17] P. Wang, J. Fang, H. Duan, and H. Li, "Compressed channel estimation for intelligent reflecting surface-assisted millimeter wave systems," *IEEE Signal Process. Lett.*, vol. 27, pp. 905–909, May 2020.

[18] J. Chen, Y.-C. Liang, H. Victor Cheng, and W. Yu, "Channel estimation for reconfigurable intelligent surface aided multi-user MIMO systems," Dec. 2019, *arXiv:1912.03619*. [Online]. Available: http://arxiv.org/abs/1912.03619

[19] A. Taha, M. Alrabeiah, and A. Alkhateeb, "Enabling large intelligent surfaces with compressive sensing and deep learning," *IEEE Access*, vol. 9, pp. 44304–44321, Mar. 2021.

[20] A. M. Elbir, A. Papazafeiropoulos, P. Kourtessis, and S. Chatzinotas, "Deep channel learning for large intelligent surfaces aided mm-wave massive MIMO systems," *IEEE Wireless Commun. Lett.*, vol. 9, no. 9, pp. 1447–1451, Sep. 2020.

[21] Z. Wan, Z. Gao, and M.-S. Alouini, "Broadband channel estimation for intelligent reflecting surface aided mmWave massive MIMO systems," in *Proc. IEEE Int. Conf. Commun. (ICC)*, Dublin, Ireland, Jun. 2020, pp. 1–6.

[22] X. Wei, D. Shen, and L. Dai, "Channel estimation for RIS assisted wireless communications: Part I—Fundamentals, solutions, and future opportunities (invited paper)," *IEEE Commun. Lett.*, vol. 25, no. 5, pp. 1398–1402, May 2021.

[23] X. Wei, D. Shen, and L. Dai, "Channel estimation for RIS assisted wireless communications: Part II—An improved method based on double-structured sparsity (invited paper)," *IEEE Commun. Lett.*, vol. 25, no. 5, pp. 1403–1407, May 2021.

[24] D. Shen and L. Dai, "Dimension reduced channel feedback for reconfigurable intelligent surface aided wireless communications," *IEEE Trans. Commun.*, 2021.

[25] E. Björnson and L. Sanguinetti, "Rayleigh fading modeling and channel hardening for reconfigurable intelligent surfaces," *IEEE Wireless Commun. Lett.*, vol. 10, no. 4, pp. 830–834, Apr. 2021.

[26] L. Dai *et al.*, "Reconfigurable intelligent surface-based wireless communication: Antenna design, prototyping and experimental results," *IEEE Access*, vol. 8, pp. 45913–45923, Mar. 2020.

[27] E. Ahmed and A. M. Eltawil, "All-digital self-interference cancellation technique for full-duplex systems," *IEEE Trans. Wireless Commun.*, vol. 14, no. 7, pp. 3519–3532, Jul. 2015.

[28] F. Zhu, F. Gao, T. Zhang, K. Sun, and M. Yao, "Physical-layer security for full duplex communications with self-interference mitigation," *IEEE Trans. Wireless Commun.*, vol. 15, no. 1, pp. 329–340, Jan. 2016.

[29] A. Masmoudi and T. Le-Ngoc, "Channel estimation and self-interference cancelation in full-duplex communication systems," *IEEE Trans. Veh. Technol.*, vol. 66, no. 1, pp. 321–334, Jan. 2017.

[30] D. Xu, X. Yu, Y. Sun, D. W. K. Ng, and R. Schober, "Resource allocation for IRS-assisted full-duplex cognitive radio systems," *IEEE Trans. Commun.*, vol. 68, no. 12, pp. 7376–7394, Dec. 2020.

[31] H. Shen, T. Ding, W. Xu, and C. Zhao, "Beamformig design with fast convergence for IRS-aided full-duplex communication," *IEEE Commun. Lett.*, vol. 24, no. 12, pp. 2849–2853, Dec. 2020.

[32] A. Kumar and S. Aniruddhan, "A 2.35 GHz cross-talk canceller for 2×2 MIMO full-duplex wireless system," in *IEEE MTT-S Int. Microw. Symp. Dig.*, Boston, MA, USA, Jun. 2019, pp. 877–880.

[33] S. Atapattu, R. Fan, P. Dharmawansa, G. Wang, J. Evans, and T. A. Tsiftsis, "Reconfigurable intelligent surface assisted two–way communications: Performance analysis and optimization," *IEEE Trans. Commun.*, vol. 68, no. 10, pp. 6552–6567, Oct. 2020.

[34] X. Gao, L. Dai, Y. Sun, S. Han, and I. Chih-Lin, "Machine learning inspired energy-efficient hybrid precoding for mmWave massive MIMO systems," in *Proc. IEEE Int. Conf. Commun. (ICC)*, Paris, France, May 2017, pp. 1–6.

Chen Hu received the B.E. degree in electronic engineering from Tsinghua University, Beijing, China, in 2016, where he is currently pursuing the Ph.D. degree in electronic engineering. His research interests include sparse signal processing, mmWave massive MIMO, and reconfigurable intelligent surfaces (RIS), with the emphasis on channel estimation. He has received the Freshman Scholarship of Tsinghua University in 2012, the Excellent Thesis Award of Tsinghua University in 2016, the IEEE Transactions on Communications Exemplary Reviewer Award in 2018, and the National Scholarship in 2020.

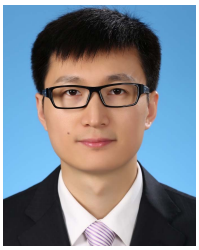

Linglong Dai received the B.S. degree from Zhejiang University, Hangzhou, China, in 2003, the M.S. degree (Hons.) from the China Academy of Telecommunications Technology, Beijing, China, in 2006, and the Ph.D. degree (Hons.) from Tsinghua University, Beijing, in 2011.

From 2011 to 2013, he was a Post-Doctoral Research Fellow with the Department of Electronic Engineering, Tsinghua University, where he was an Assistant Professor from 2013 to 2016 and has been an Associate Professor since 2016. He has coauthored the book *MmWave Massive MIMO: A Paradigm for 5G* (Academic Press, 2016). He has authored or coauthored over 60 IEEE journal articles and over 40 IEEE conference papers. He also holds 19 granted patents. His current research interests include reconfigurable intelligent surface (RIS), massive MIMO, millimeter-wave/terahertz communications, and machine learning for wireless communications.

He has received five IEEE Best Paper Awards from the IEEE ICC 2013, the IEEE ICC 2014, the IEEE ICC 2017, the IEEE VTC 2017-Fall, and the IEEE ICC 2018. He has also received the Tsinghua University Outstanding Ph.D. Graduate Award in 2011, the Beijing Excellent Doctoral Dissertation Award in 2012, the China National Excellent Doctoral Dissertation Nomination Award in 2013, the URSI Young Scientist Award in 2014, the IEEE Transactions on Broadcasting Best Paper Award in 2015, the Electronics Letters Best Paper Award in 2016, the National Natural Science Foundation of China for Outstanding Young Scholars in 2017, the IEEE ComSoc Asia-Pacific Outstanding Young Researcher Award in 2017, the IEEE ComSoc Asia-Pacific Outstanding Paper Award in 2018, the China Communications Best Paper Award in 2019, the IEEE Access Best Multimedia Award in 2020, and the IEEE Communications Society Leonard G. Abraham Prize in 2020. He was listed as a Highly Cited Researcher by Clarivate Analytics in 2020. He is an Area Editor of IEEE COMMUNICATIONS LETTERS, and an Editor of IEEE TRANSACTIONS ON COMMUNICATIONS and IEEE TRANSACTIONS ON VEHICULAR TECHNOLOGY. Particularly, he is dedicated to reproducible research and has made a large amount of simulation codes publicly available.

Shuangfeng Han received the Ph.D. degree in electronic engineering from Tsinghua University in 2006. He is the Principal Member of Technical Staff and a fellow of the China Mobile Research Institute. His research interests include massive MIMO, NOMA, EE-SE co-design, MIMO for high speed trains, artificial intelligence empowered networks, and air interfaces design. He was a recipient of the IEEE Comsoc 2018 Fred W. Ellersick Award and the IEEE Comsoc AP Outstanding Paper Award.

Xiaoyun Wang is currently the Technical Leader in the overall research and development of mobile communication networks in China. She has been committed to the research of technology strategy, system architecture, and networking technology for many years. She presided over three national major network projects in 3G, 4G, and 5G, and made outstanding contributions. Her research interests include technology strategy, system architecture, and networking technology. She is an Alternate Member of the Political Bureau of the CPC Central Committee, and the General Manager of the Technology Department, China Mobile. She was a recipient of special prize of the National Science and Technology Progress Award (ranking No. 2), first prize (ranking 5), 16 provincial and ministerial awards, and the first National Innovation and Excellence Award, the Chinese Youth Science and Technology Award. She was also selected in "one billion Talents Project in the new century."